IFA - 94/36 Sep. 1994

AARHUS-ASTRO-1994-11 ISSN 0906-3870

IMPROVED *I*-BAND CCD PHOTOMETRY OF NGC 3379 AND COMPARISON WITH A VIOLENT RELAXATION MODEL

M. Sodemann and B. Thomsen

Fermilab Library
0 1160 0054652 7

-ERMILAB
DEC 27 199
IBRAR

Inst. of Physics and Astronomy
University of Aarhus
DK-8000 Aarhus C
Denmark

Accepted by: Astronomy and Astrophysics.

A&A manuscript no.
(will be inserted by hand later)

Your thesaurus codes are:
03(11.05.1; 11.09.1 NGC 3379; 11.16.1; 11.19.6)

ASTRONOMY AND ASTROPHYSICS
15.9.1994

Improved I–band CCD photometry of NGC 3379 and comparison with a violent relaxation model*

Marianne Sodemann and Bjarne Thomsen

Institut for Fysik og Astronomi, Aarhus Universitet, DK-8000 Aarhus C, Denmark

Received 19 May 1994 / Accepted 8 July 1994

Abstract. We have obtained the E–W surface brightness profile of the standard elliptical NGC 3379 from overlapping NTT/SUSI frames out to $\sim 5'.2$ from the centre of the galaxy. These observations in I include a high-resolution frame ($\sigma_* = 0''.37$) of the centre. We find that a single isothermal core does not fit the central surface photometry of this galaxy, indicating that NGC 3379 may be the result of a more complex formation scenario than a dissipationless collapse. Combining B-band literature data with the present I-band profile we obtain a colour gradient consistent with an average abundance gradient of $\Delta[\mathrm{Fe/H}]/\Delta \log R = -0.21 \pm 0.03$.

Key words: galaxies: ellipticals – galaxies: photometry – galaxies: structure – galaxies: NGC 3379

1. Introduction

NGC 3379 is one of the best-observed elliptical galaxies and as such known as a luminosity standard (Trans. IAU 1961). Due to its relative proximity NGC 3379 is often mentioned when resolution and central brightness profiles are discussed.

In the literature different models, all with an isothermal centre, for elliptical galaxies have been presented and compared with observations: In a photographic/photoelectric B-band study of NGC 3379 de Vaucouleurs & Capaccioli (1979) find a deviation from King's formula (King 1962), and they conclude that King's profile fails to describe the excess of light near the centre of giant ellipticals. Based on V-band CCD photometry Kormendy (1985a) reaches the same conclusion, namely that the core profile of NGC 3379 is not consistent with an isothermal model. However, a model that reproduces de Vaucouleurs' $R^{1/4}$ law and fits the B-band surface photometry of NGC 3379 remarkably well is presented in Hjorth & Madsen (1991) (hereafter referred to as HM). We compare our I-band profile with the model of HM and find it difficult to fit the I-band profile with this model. Worthey (1994) recommends I-band observations for studies in which the property that light traces stellar mass is desirable, as his I-band model data are nearly independent of metal abundance. This is clearly of importance here where we compare photometric observations with a dynamical model. The difference in the B-band and I-band observations is expressed in a colour gradient.

It is known that the resolution of the central region of elliptical galaxies is very sensitive to the seeing conditions under which the observations were made (Schweizer 1979, 1981). Corrections for these seeing effects are made by Kormendy (1985b) and Lauer (1985a,b). Their results compare well, in that they show that isothermal cores are rare. Møller et al. (1993) find no resolved isothermal cores in their sample of elliptical galaxies (not including NGC 3379), also implying that isothermal cores are rare. NGC 3379 is one of four elliptical galaxies investigated by van der Marel et al. (1990). They find that the rotation curves rule out isotropic velocity dispersion tensors, and an anisotropic model, in which the tangential velocity dispersion exceeds those in the radial and vertical directions, provides an acceptable fit to the observations. The coupling of CCD exposures ($\sigma_* = 0''.97$) and Schmidt plates was used by Capaccioli et al. (1990) to map the B-band luminosity distribution of NGC 3379. We compare our surface brightness profile in I with this and newly published CCD surface photometry ($\sigma_* = 0''.50$) obtained by Goudfrooij et al. (1994).

2. Observations and Reductions

The data presented here were obtained in 1993 April with the NTT/SUSI, La Silla. The exposure times were 24×300 s in I (~ 8250 Å) and 1×500 s in V (~ 5400 Å). The chip was the TEK-1024 (24 μm square pixels) with rms RON = 2.3 ADU, conversion factor = 3.3 e^-/ADU and $0''.134$ per pixel at the Nasmyth focus giving a field of $2'.3 \times 2'.3$. The seeing was good, varying between $0''.8$ and $1''.2$ FWHM ($= 2.35\sigma_*$). To remove the effects of bad pixels and residual flat-field non-uniformity the frames of the centre made up a mosaic, each frame shifted slightly, approximately $6''$, relative to the previous one.

For the data reductions a local image handling program was used. A median of 13 bias frames was calculated and this bias frame and the individual residual bias level were then subtracted from each frame. The flat-field was a difference between a high charge level exposure of the twilight sky and a corresponding low-level exposure through the same filter. This step is used in order to eliminate any low-level non-linearity in the flat-field exposure. Each frame was then divided by the normalized flat-field. Residual errors due to flat-fielding are less

* Based on observations made with the European Southern Observatory's New Technology Telescope, La Silla, Chile.

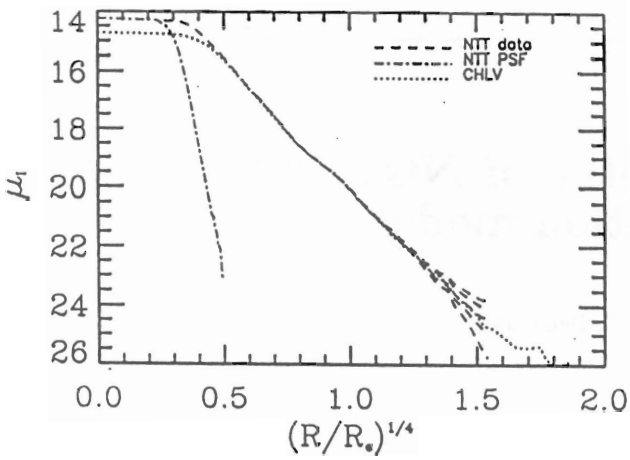

Fig. 1. Surface brightness profile μ_I of NGC 3379 together with that of CHLV in B shifted by $B - I = 2.17$. Effects on the background sky level of ± 1 ADU and ± 2 ADU are indicated. $R_e = 53''.1$ for the E–W axis

than 0.3 % of the sky background. Cosmic ray events were removed by a routine which detects and replaces the cosmic rays by fitting a sum of polynomial terms in a square region centred on any suspected spike.

The standard stars of the 'dipper asterism' in M67 (Schield 1983) were observed to derive the colour term, and the zero-point was determined by aperture photometry of the galaxy (Burstein et al. 1987). The precision of our photometry is $0^m.03$, uncertainties added in quadrature, with the major contribution from the photometry of Burstein et al. (1987).

5 out of the 24 CCD frames in I form part of the galaxy's E–W profile and cover the galaxy down to $\mu_I = 24.42$ mag arcsec^{-2} or $5'.24$ from the galaxy centre. The profile shown in Fig. 1 is composed of this E–W profile and a central frame with $\sigma_* = 0''.37$ covering the galaxy centre. A revised version of the galaxy fitting routine described in Thomsen & Baum (1989) was applied to our data. Our routine is developed to obtain a smooth fit of a galaxy rather than a fit to isophotes, and it calculates radial harmonic profiles by means of a robust regression technique that fits Fourier series to elliptical rings centred on the object. The routine allows fits to incomplete ellipses, e.g. the present series of E–W orientated overlapping frames. At a distance of $R_e = 53''.1$ (see later) from the galaxy centre the accidental errors in the profile fit are less than 0.05 % of the galaxy signal. The fitting routine applied to the central image resulted in a smooth image, and the difference between the central image and a smooth fit is shown in Fig. 2.

In general the sky in I varies rapidly (up to 5 % between subsequent exposures of this data set). Therefore blank sky exposures, preceding and following each galaxy exposure, would be improper to use for background removal, besides being time-consuming. Instead we obtained, within less than an hour at the meridian, a long-ranging series of overlapping frames. During an observing run this procedure for obtaining the sky background only has to be done once for each target galaxy. We tacitly assumed that the extinction (as well as the surface brightness of the galaxy) were unchanged and that we would reach the sky background. The series consists of 5 frames, which are numbered consecutively from the innermost frame and outwards. Then, working inwards from the outermost frame of the series, we determined the sky background for each galaxy exposure in the following way: In each frame the observed signal is the sum of the galaxy signal and sky background. However, in the farthest corner of the fifth frame we adopt the sky background μ_I^5(sky) as the only contribution. The difference of the observed signal and the sky background in a small patch within the overlapping region between the fifth and fourth frame determines the surface brightness μ_I^5 at that place. In the overlapping region we now have μ_I^5, which is equal to μ_I^4 under the assumption of non-changing extinction. The difference between the observed signal and μ_I^4 in the small patch gives μ_I^4(sky). This is repeated for each overlapping region until μ_I^1(sky) and μ_I^1 for the innermost frame is obtained. We thereby have μ_I, and μ_I(sky), within a specific area common to each frame of the galaxy centre. Changing the sky by ± 1 ADU changes μ_I(sky) by ∓ 0.003 and this is seen as the truncation and the flattening, respectively, of the light profile in Fig. 1. The assumption that the extinction remains constant during the series is correct within $0^m.03$. The accidental errors in the outermost part of the profile fit are less than 0.2 % of the galaxy signal.

To check the accuracy of our photometric results on NGC 3379 we made a comparison with the E–W profile obtained by Capaccioli et al. (1990) (hereafter referred to as CHLV). For the comparison we assumed there was no colour gradient in $B - I$ present and adopted the value $B - I = 2.17$ from Goudfrooij et al. (1994). No systematic errors (Capaccioli & de Vaucouleurs 1983) are seen in Fig. 1. Deviations between the two profiles in the core region will be discussed.

The observations presented here are part of a larger data sample obtained with the NTT and the Nordic Optical Telescope, La Palma. The data were obtained as part of a programme aimed at using Surface Brightness Fluctuation (SBF) measurements as an indicator of differencies in the stellar population of elliptical galaxies, and we use NGC 3379 to test our reduction methods (Thomsen & Sodemann 1993). The derivation of the SBF signal requires a smooth fit to the galaxy and a proper determination of the background sky level. These two requirements have been fulfilled and are as such presented here as a provisional result towards SBF measurements.

3. Analysis and Results

The most convenient fitting function for galaxy spheroids (Kormendy 1977) is the de Vaucouleurs' (1948) $R^{1/4}$ law (see also Caon et al. 1993). In HM an isotropic equilibrium distribution function was presented, which reproduces the $R^{1/4}$ law. This model, based on violent relaxation, has as its only free parameter the dimensionless central potential Ψ_0. It was shown by HM that for their model the residuals from the $R^{1/4}$ law give an excellent fit to the surface photometry of NGC 3379 obtained by CHLV. As such, the model described the observed 'waves' in the residuals, not as a marker of additional components or modifications in the radial distribution of light induced by effects of a given environment, but reflecting the physics behind the model: violent relaxation resulting in an isothermal core for the inner region, and for the outer region $\rho(r) \sim r^{-(\eta+3/2)}$, where $2.6 < \eta < 2.9$ in the relevant range of values of Ψ_0.

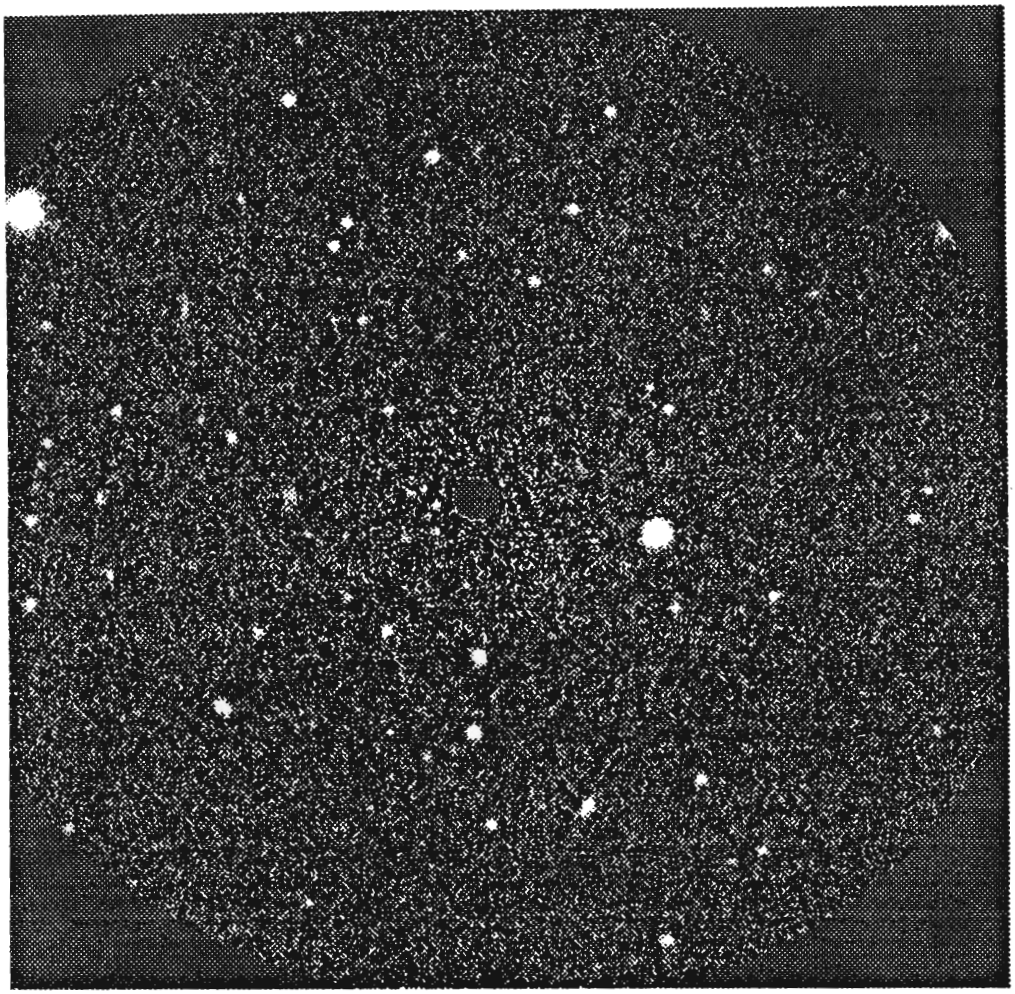

Fig. 2. The difference of the central image of NGC 3379 and a smooth fit. The galaxy fitting routine (see text) leaves the galaxy unaffected outside the chosen range of the fit. The outer radius of the fit extends outside the boundaries of the image. North is up, East is left, and the field is 2.'3 × 2.'3. Objects are foreground stars, background galaxies and globular clusters. The bright star to the right of the centre is used as PSF star ($\sigma_* = 0.''37$). Note that no systematic unwanted residual structures are present

We want to compare the model of HM with our observations, which are of higher resolution ($\sigma_* = 0.''37$) than the data of CHLV ($\sigma_* = 0.''97$). The comparison is carried out by performing a convolution of the Point Spread Function (PSF) and images reconstructed from the one-dimensional model profiles. Our observations of NGC 3379 included simultaneous sampling of a bright PSF star within the central image.

We assume (Thomsen & Frandsen 1983) that the shape of the Optical Transfer Function (OTF) can be represented by

$$\begin{aligned} OTF(u,v) &= aH(\omega)\exp(-2\pi i\theta) \\ \theta &= \alpha u + \beta v \\ H(\omega) &= \exp(-(\omega/\gamma)^P) \\ \omega^2 &= u^2 + v^2 + a_2(u^2 - v^2) + 2b_2 uv \end{aligned}$$

where a, α, β, γ, P, a_2 and b_2 are determined by a least-squares fit to the complex Fourier transform of the PSF star. This functional form is found to give one of the best fits to stellar profiles (Saglia et al. 1993). It should be noted that we find $P = 1.64$ which differs from the Gaussian $P = 2$, and that the theory of turbulence predicts $P = 1.67$ (Woolf 1982). The exact location of the PSF star in the image domain is given by (α, β), and (a_2, b_2) indicates the size of any possible ellipticity as well as the direction of the ellipticity. With the obtained parameters we compute a noise free OTF, multiply it by the Fourier transform of the model and perform the Fourier transform to the image domain. For $P = 1.67$ we find γ·FWHM= 0.46, where FWHM is obtained from the PSF, which is derived through the OTF. The second derivatives of the OTF at (0, 0) diverge for $P < 2$, and hence the second moments of the PSF do not exist (Bracewell 1978).

The existence of the empirical $R^{1/4}$ luminosity law proposed by de Vaucouleurs provides the often used way to present observed (or modeled) data: The differencies $\Delta\mu$ between the observed magnitudes along a preferred axis and the $R^{1/4}$ law for the corresponding parameters R_e and μ_e are plotted.

We now plot a one-dimensional radial cut in the seeing convolved two-dimensional model, subtract the $R^{1/4}$ law and compare with the residuals of our E–W profile, see Fig. 3. We find that for none of the selected central potentials $\Psi_0 = 12, 11, 10$ and 9.75 will the seeing convolved model of HM fit our data. The model cannot simultaneously fit the inner and outer part of the data around $(R/R_e)^{1/4} \simeq 0.5$.

In order to estimate the total magnitude I_T, and thereby R_e, we extend our E–W profile with the $R^{1/4}$ law. The growth curve $I_T(R)$ is then determined by a numerical integration of the extended E–W light profile. If a Keplerian potential $\Psi(r) \sim r^{-1}$ is adopted for the outer region of the galaxy, the model of HM implies $\rho(r) \sim r^{-4}$ for $\eta = 2.5$. The model, for which the central potential is $\Psi_0 = 9.75$ ($\eta = 2.65$), resembles the $R^{1/4}$ law in the outer region. Two simple integrations show

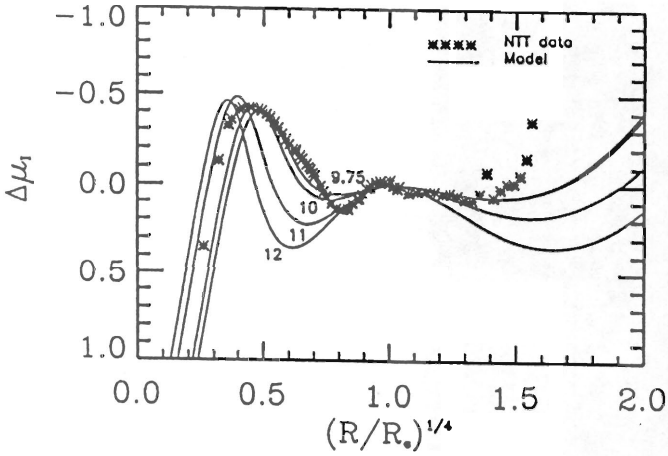

Fig. 3. Residuals $\Delta\mu_I$ from the $R^{1/4}$ law for four seeing convolved models and the observed light profile. Numbers next to the curves are the values of the central potential Ψ_0. For $(R/R_e)^{1/4} \lesssim 1.2$ the accuracy of the observations are better than ± 0.03 and for $1.3 \lesssim (R/R_e)^{1/4} \lesssim 1.5$ better than ± 0.2

that *if* the density goes as $\rho(r) \sim r^{-4}$ for the outer region then the growth curve $I_T(R) \sim R^{-1}$. The growth curve of the $R^{1/4}$ law (Thomsen & Frandsen 1983) fits the observed growth curve remarkably well, and we find the linear dependence when $I_T(R)$ is plotted as a function of R^{-1}. The intersection of $I_T(R)$ for $R^{-1} \to 0$ gives I_T. We estimate the total magnitude $I_T = 8.01 \pm 0.05$ and the E–W effective radius $R_e = 53''.1 \pm 4''.0$. This gives $a_e = 55''.8 \pm 4''.2$ for the effective semimajor axis in I ($a_e = 56''.8 \pm 3''.8$ in B, see CHLV), based on a determination of the mean major axis position angle $PA = 72°$. Uncertainty in the determination of the intersection of $I_T(R)$ for $R^{-1} \to 0$ gives rise to the uncertainty stated. Correction for Galactic absorption and K-correction is adopted from Goudfrooij et al. (1994) and equals 0.03.

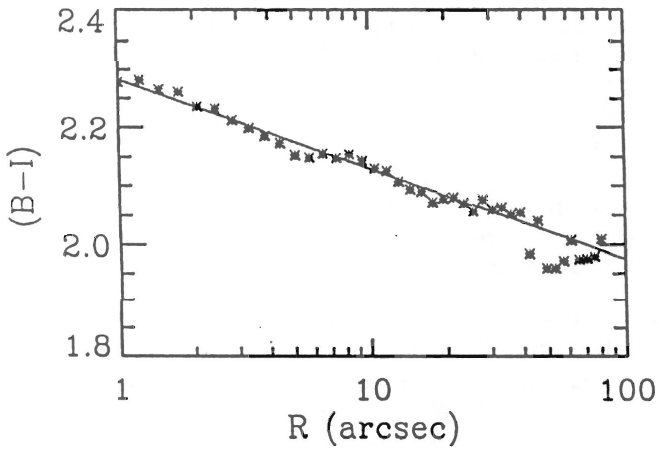

Fig. 4. Colour gradient obtained by the present light profile in I and that of CHLV in B. The line is a least-squares fit to the observations and gives $\Delta(B-I)/\Delta \log R = -0.15 \pm 0.02$

We then degraded our profile ($\sigma_* = 0''.37$) to the resolution present in the data of CHLV ($\sigma_* = 0''.97$). Because of the small ellipticity ($\epsilon \simeq 0.10$) of NGC 3379 we made a rotationally symmetric equivalent of our E–W profile. The higher-resolution data were convolved by the use of an OTF with an equivalent 'dispersion' of $\sigma_* = (0''.97^P - 0''.37^P)^{1/P} = 0''.85$, where we have adopted $P = 1.67$ (turbulence theory) for both data sets. The two E–W profiles, CHLV's in B and ours in I, still do not match after degradation of the latter. We interpret this as due to the presence of a colour gradient in $B-I$. The average E–W colour gradient (see Fig. 4) between $1''.0$ and $39''.1$ is $\Delta(B-I)/\Delta \log R = -0.15 \pm 0.02$. Again, uncertainties from sky background removal, flat-fielding, and the photometry of CHLV are added in quadrature. Changing P from 1.67 to 2 (Nieto 1983) in the calculation of σ_* above flattens the gradient by 0.02. We find for the E–W profile $\overline{B-I} = 2.14 \pm 0.04$ within $R_e/2 = 26''.5$, when $R_e = 53''.1$. Goudfrooij et al. (1994) find $\Delta(B-I)/\Delta \log R = -0.10 \pm 0.01$ for the colour gradient and $\overline{B-I} = 2.17 \pm 0.00$ within $R_e/2 = 17''.7$, adopting a significantly different value $R_e = 35''.3$ for the semimajor axis.

In addition, we have compared a degradation of the model of HM with our degraded profile in I, both matching the resolution of CHLV. The fact that the model fits the B-band profile of CHLV but not the I-band profile is due to the colour gradient, not the difference in resolution.

The stellar population models of Worthey (1994) implies an average abundance gradient of $\Delta[\mathrm{Fe/H}]/\Delta \log R = -0.21 \pm 0.03$ for a colour gradient of $\Delta(B-I)/\Delta \log R = -0.15 \pm 0.02$. This estimate is based on the assumption that the colour gradient is due to a metallicity gradient only. Line-strengths of Mg_2 and a mean of Fe5270 and Fe5335 (Davies et al. 1993) give the average abundance gradients $\Delta[\mathrm{Fe/H}]/\Delta \log R = -0.29 \pm 0.01$ and $\Delta[\mathrm{Fe/H}]/\Delta \log R = -0.30 \pm 0.06$, respectively, again using the calibration of Worthey (1994). The gradient obtained by the Mg_2 index is significantly steeper than the one obtained by our colour gradient, possibly indicating a non-constant [Mg/Fe] ratio. Worthey (1994) also presents fluctuation magnitudes from which we read that the changes in the fluctuation magnitudes $\bar{I}$ and $\bar{V}$ are very similar, whereas a weakening of $\bar{I}$ towards the centre of the galaxy is accompanied by a brightening in $\bar{K}$. We have estimated $\Delta\bar{I}/\Delta \log R \sim -0.5$ and $\Delta\bar{K}/\Delta \log R \sim 0.1$ from our colour gradient and the stellar population models.

Table 1. I-band CCD photometry of NGC 3379

Parameter	Value
R_e E–W axis	$53''.1 \pm 4''.0$
μ_e E–W axis	20.09 ± 0.03
a_e semimajor axis	$55''.8 \pm 4''.2$
I_T total magnitude	8.01 ± 0.05
$\Delta(B-I)/\Delta \log R$ colour gradient	-0.15 ± 0.02
$\overline{B-I}$ within $R_e/2$	2.14 ± 0.04

4. Conclusion

We have presented the I-band surface brightness profile of NGC 3379 obtained from a long-ranging series of high-resolu-

tion CCD observations. Our photometric results are listed in Table 1.

We find that the model introduced by Hjorth & Madsen (1991) has difficulties in reproducing the observed light profile in I. This reinforces the findings of de Vaucouleurs & Capaccioli (1979) and Kormendy (1985a) that the centre of NGC 3379 is more complex than the presence of a single isothermal core. From HST observations (not including NGC 3379) Crane et al. (1993) conclude that none of the galaxies in their sample show isothermal cores. The difference in I and B is most likely due to the colour gradient suppressing the centre of the galaxy seen in B. The colour gradient reflects a change in the stellar population, which makes a constant mass-to-light ratio impossible. Observational evidence like abundance gradients (Davies et al. 1993) and high central densities (Kormendy 1989) point in the direction that dissipation has played a role in the formation of elliptical galaxies. If dissipation is taken into account, then deviations from a single isothermal centre may be expected, as successive generations of stars are likely to have different isothermal properties. As stated in HM, and in Hjorth & Madsen (1993) where anisotropy is incorporated in their model, dissipation in elliptical galaxy formation seems to be needed. Capaccioli et al. (1991) find indications of a disc (viewed face-on) in NGC 3379. However, this will hardly affect the core region where we find the disagreement between the observed light profile and the model.

Acknowledgements. We wish to thank Jes Madsen for useful comments and Jens Hjorth for providing the model data and constructive discussions.

References

Bracewell R.N., 1978, The Fourier Transform and its Applications. McGraw-Hill
Burstein D., Davies R.L., Dressler A., Faber S.M., Stone R.P.S., Lynden-Bell D., Terlevich R.J., Wegner G., 1987, ApJS 64, 601
Caon N., Capaccioli M., D'Onofrio M., 1993, MNRAS 265, 1013
Capaccioli M., de Vaucouleurs G., 1983, ApJS 52, 465
Capaccioli M., Held E.V., Lorenz H., Vietri M., 1990, AJ 99, 1813 (CHLV)
Capaccioli M., Vietri M., Held E.V., Lorenz H., 1991, ApJ 371, 535
Crane P., et al., 1993, AJ 106, 1371
Davies R.L., Sadler E.M., Peletier R.F., 1993, MNRAS 262, 650
de Vaucouleurs G., 1948, Ann. Ap., 11, 247
de Vaucouleurs G., Capaccioli M., 1979, ApJS, 40, 699
Goudfrooij P., Hansen L., Jørgensen H.E., Nørgaard-Nielsen H.U., de Jong T., van den Hoek L.B., 1994, A&AS 104, 179
Hjorth J., Madsen J., 1991, MNRAS 253, 703 (HM)
Hjorth J., Madsen J., 1993. In: Danziger I. J., Zeilinger W. W., Kjär K. (eds.) Structure, Dynamics and Chemical Evolution of Elliptical Galaxies. ESO Conference and Workshop Proceedings No. 45, p. 263
King I., 1962, AJ 67, 471
Kormendy J., 1977, ApJ 218, 333
Kormendy J., 1985a, ApJ 292, L9
Kormendy J., 1985b, ApJ 295, 73
Kormendy J., 1989, ApJ 342, L63
Lauer T.R., 1985a, ApJS 57, 473
Lauer T.R., 1985b, ApJ 292, 104
Møller P., Stiavelli M., Zeilinger W.W., 1993 In: Danziger I. J., Zeilinger W. W., Kjär K. (eds.) Structure, Dynamics and Chemical Evolution of Elliptical Galaxies. ESO Conference and Workshop Proceedings No. 45, p. 131
Nieto J.-L., 1983, A&AS 53, 383
Saglia R.P., Bertschinger E., Baggley G., Burstein D., Colless M., Davies R.L., McMahan R.K. Jr, Wegner G., 1993, MNRAS 264, 961
Schield R.E., 1983, PASP 95, 1021
Schweizer F., 1979, ApJ 233, 23
Schweizer F., 1981, AJ 86, 662
Thomsen B., Baum W.A., 1989, ApJ 347, 214
Thomsen B., Frandsen S., 1983, AJ 88, 789
Thomsen B., Sodemann M., 1993. In: Danziger I. J., Zeilinger W. W., Kjär K. (eds.) Structure, Dynamics and Chemical Evolution of Elliptical Galaxies. ESO Conference and Workshop Proceedings No. 45, p. 547
Trans. IAU, 1961, Sadler D. H. (ed), Vol. XIB, p. 304
van der Marel R.P., Binney J., Davies R.L., 1990, MNRAS 245, 582
Woolf N.J., 1982, ARA&A 20, 367
Worthey G., 1994, ApJS (in press)